Design of an Intraoral Dipole Antenna for Dental Applications

Ali Caglar Özen*, Djaudat Idiyatullin, Gregor Adriany, Steve Jungst, Naoharu Kobayashi, Beth R. Groenke, Michael Bock, Michael Garwood, Donald R. Nixdorf

*A. C. Özen and Michael Bock are with the Dept. of Radiology, Medical Physics, Medical Center – University of Freiburg, Faculty of Medicine, University of Freiburg, Freiburg, Germany. A. C. Özen is also with the German Consortium for Translational Cancer Research Partner Site Freiburg, German Cancer Research Center (DKFZ), Heidelberg, Germany, and he was with the Division of TMD & Orofacial Pain, School of Dentistry, University of Minnesota, Minneapolis, MN, USA as a Lasby Fellow in 2019 (correspondence e-mail: a.oezen@uniklinik-freiburg.de).
D. Idiyatullin, G. Adriany, S. Jungst, N. Kobayashi, M. Garwood are with the Center for Magnetic Resonance Research and Department of Radiology, University of Minnesota, Minneapolis, MN, USA.
B. R. Groenke and D. R. Nixdorf are with the Division of TMD & Orofacial Pain, School of Dentistry, University of Minnesota, Minneapolis, MN, USA. D. R. Nixdorf is also with the Department of Neurology and Radiology, Medical School, University of Minnesota, Minneapolis, MN, USA.

Index Terms: Dental MRI, Dipole Antenna, Intraoral Coil, Magnetic Resonance Imaging, Radiofrequency Coil

Supplementary Material

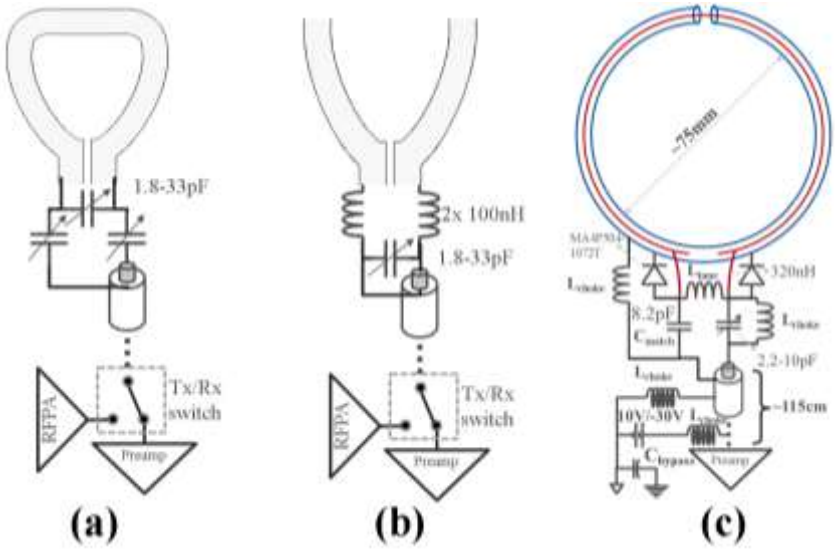

Supporting Information Figure S1: Schematics of A) loop, B) dipole and C) SLR element. Capacitive tuning and matching was implemented in the loop coil, whereas inductive tuning and capacitive matching was implemented for the dipole and the SLR coils. The loop and the dipole are interfaced to the MRI system via a Tx/Rx switch, whereas the SLR elements were interfaced via a preamplifier and a DC bias unit was coupled to the signal transmission line for active detuning.

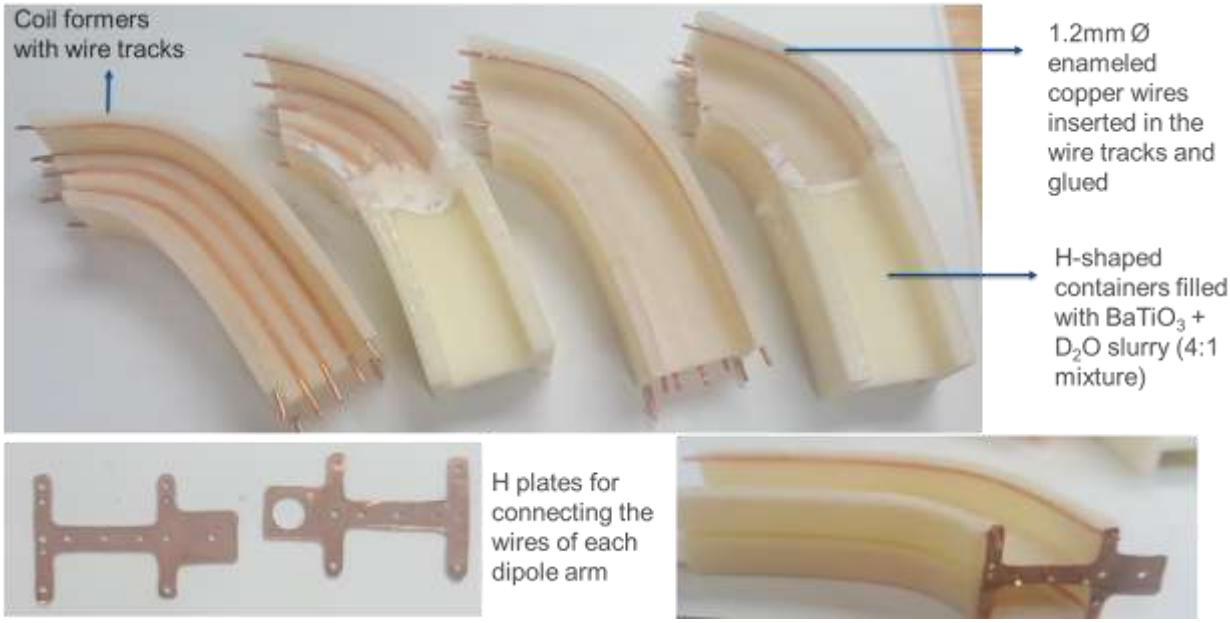

Supporting Information Figure S2: Construction steps of the multi-planar dipole with seven wires. H plates were cut out from 0.6 mm thick copper plate using a PCB milling machine.

Supporting Information Figure S3: A photo of the shielded loop resonator (SLR) array and the schematic of the tune/match interface of the SLR elements. ENVIROFLEX_178 (Huber+Suhner AG, Herisau, Switzerland) type coaxial cable was used to form SLR and to connect them to the interface circuits. Aircore inductors from Coilcraft (Cary IL) were used.

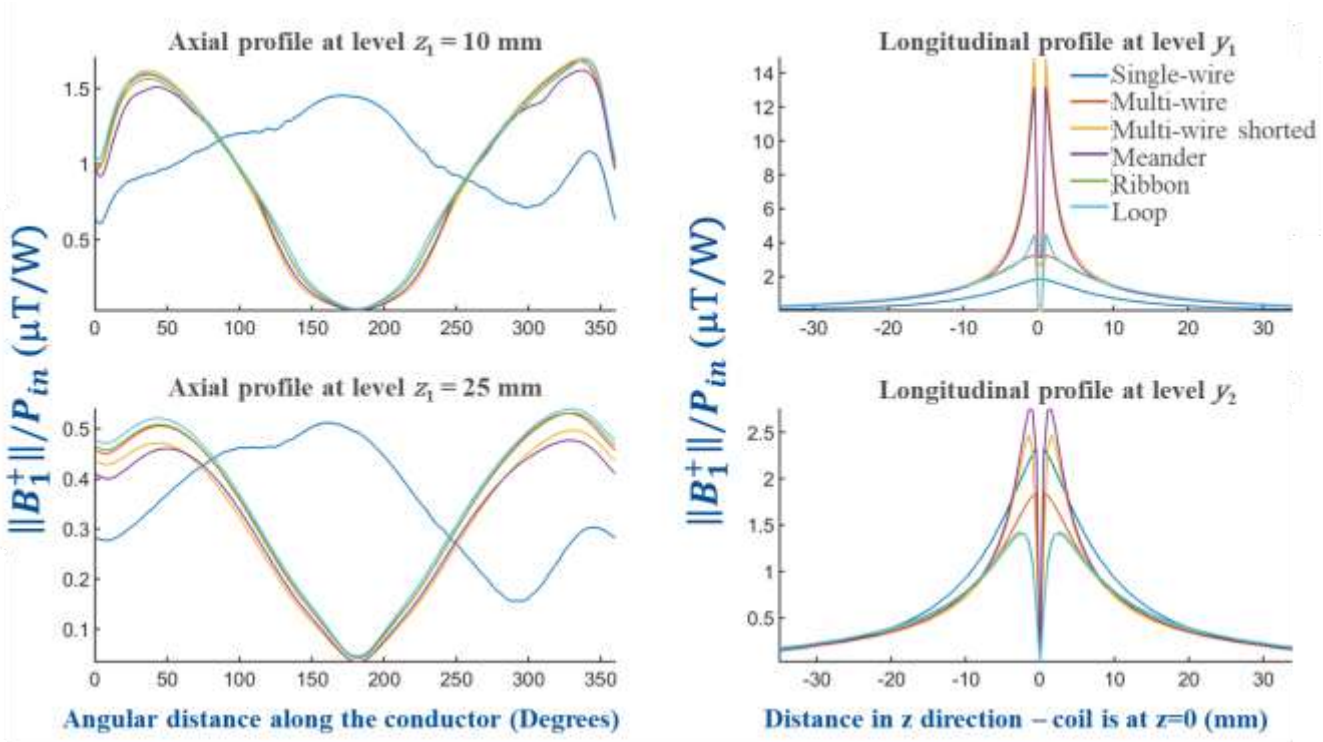

Supporting Information Figure S4: Line profiles of the planar dipoles and the reference loop coil compare $\|B_1^+\|/P_{in}$ along the tracks and levels described in Figure 1a,b.

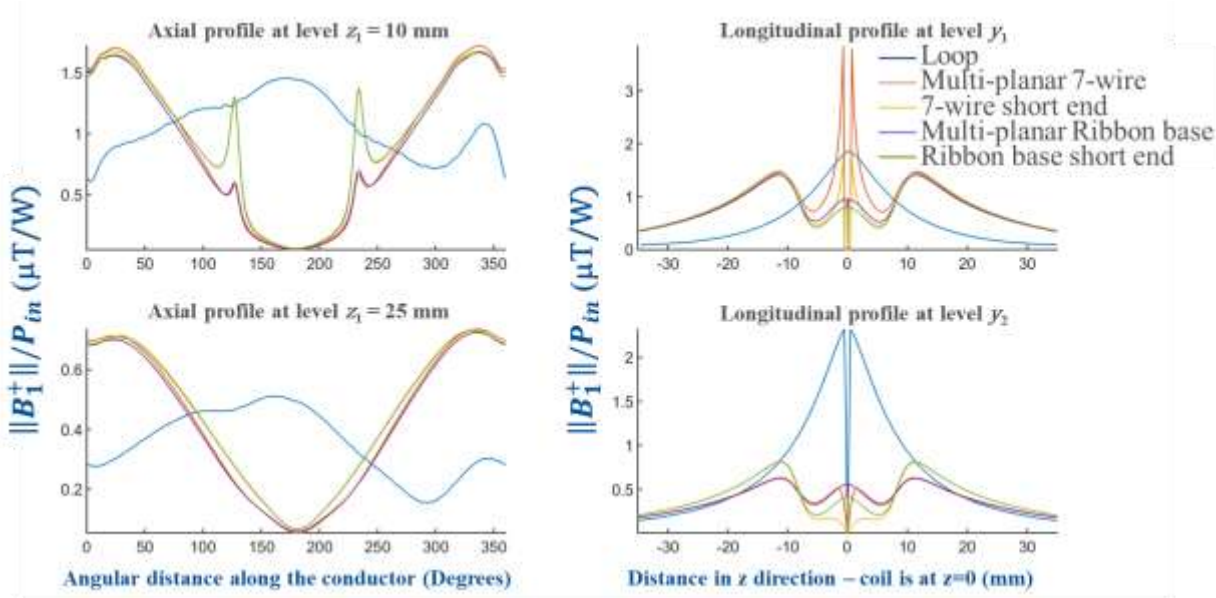

Supporting Information Figure S5: Line profiles of the multi-planar dipoles compare $\|B_1^+\|/P_{in}$ along the tracks and levels shown in Figure 1a,b.

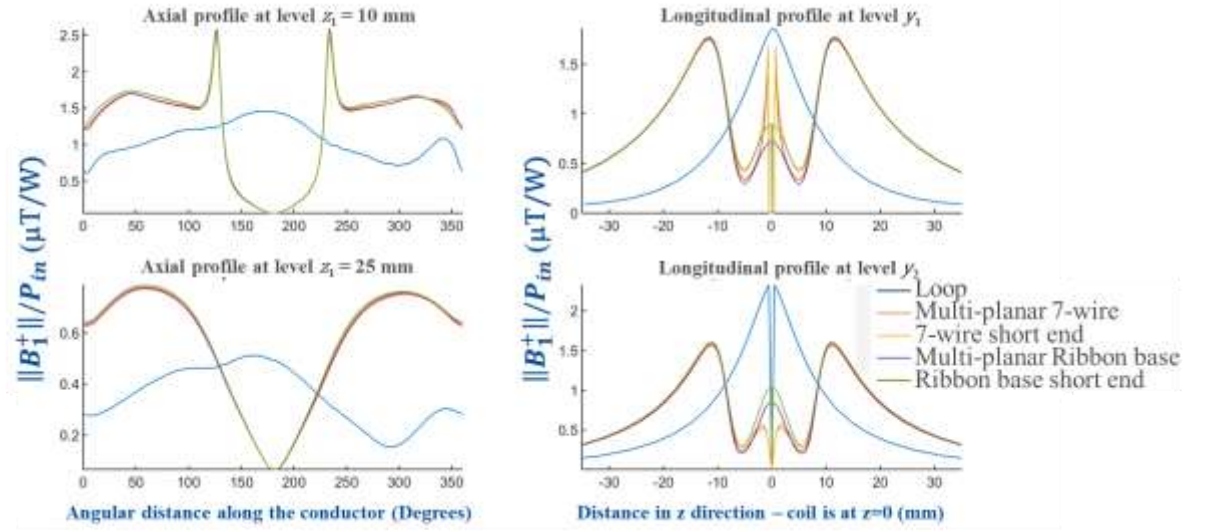

Supporting Information Figure S6: Line profiles of the multi-planar dipoles with 15 mm-long high ε_r section compare $\|B_1^+\|/P_{in}$ along the tracks and levels described in Figure 1a,b.

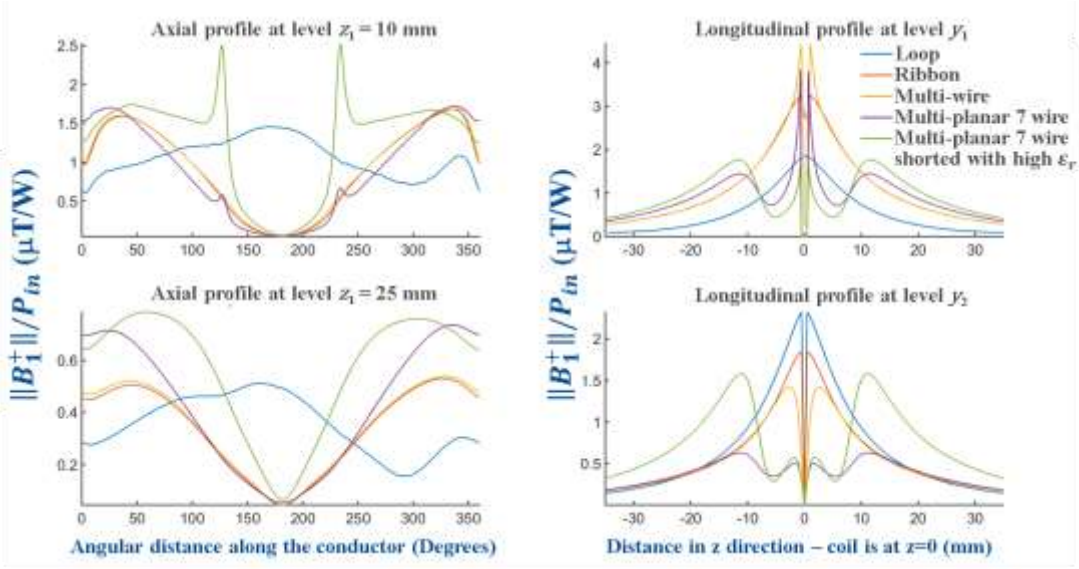

Supporting Information Figure S7: Selected line profiles along the axial curves at z = 10mm and z = 25mm planes, and longitudinal levels y_1, and y_2. Multi-planar coils with a smoother transmit efficiency line profile are favorable due to homogeneity. The longitudinal profiles shows that, the coils with higher transmit efficiency at z = 25mm , are more likely to be sensitive to signal from the roots.

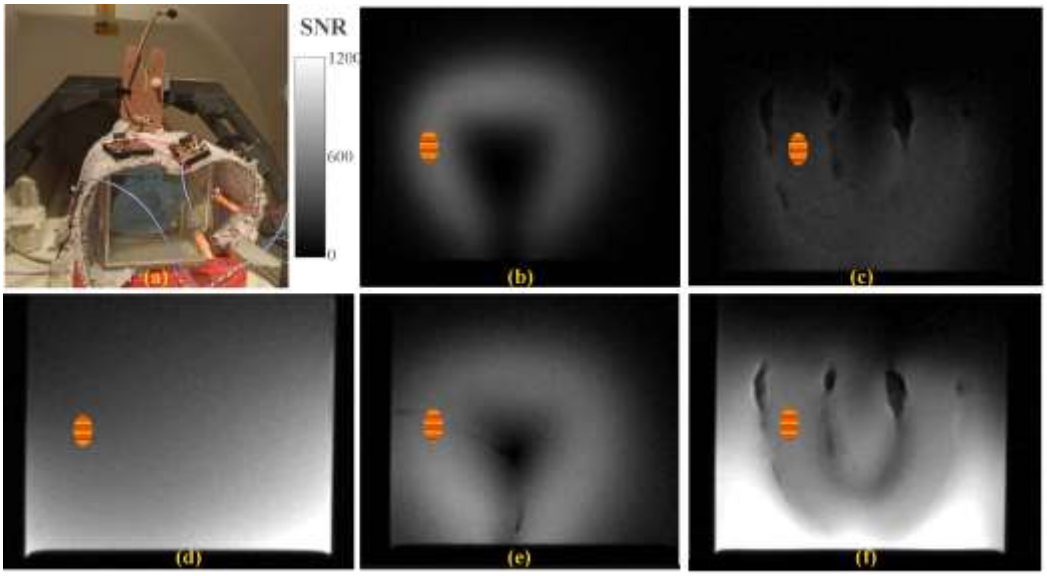

Supporting Information Figure S8: A photo of the phantom measurement setup (a). SNR maps at z = 10mm away from the coil planes obtained from phantom measurements for intraoral (b) loop, (c) dipole, (d) extraoral SLR only, and SLR combined with (e) loop and (f) dipole in Tx mode. The elliptic region of interest on the images are used for SNR comparison. SLR combined with the intraoral coils provides higher SNR. Dipole, when used as a Tx/Rx coil, has lower SNR, as a result of low Q factor.

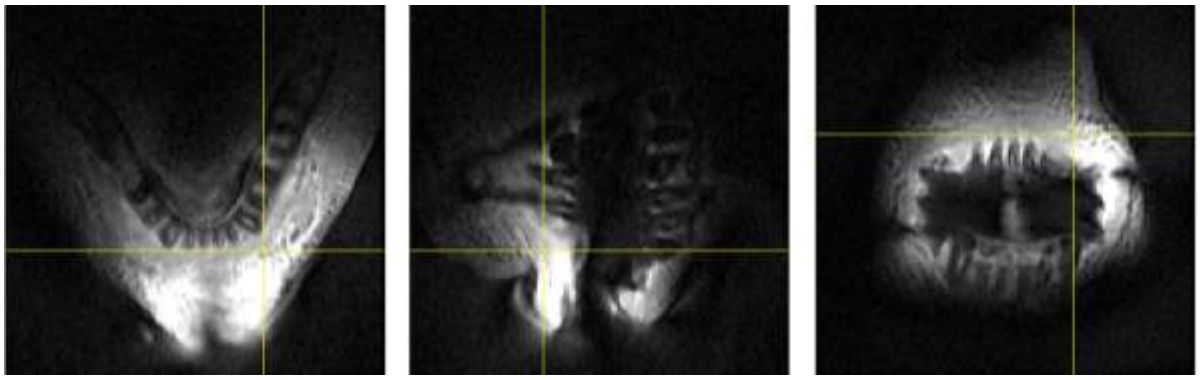

Supporting Information Figure S9: In vivo UTE image slices from three orthogonal planes. FOV of 110mm^2 was implemented. Isotropic nominal resolution of (0.86)^3 mm^3 was achieved in 8:41 min:s with a flip angle of $\alpha = 6°$.

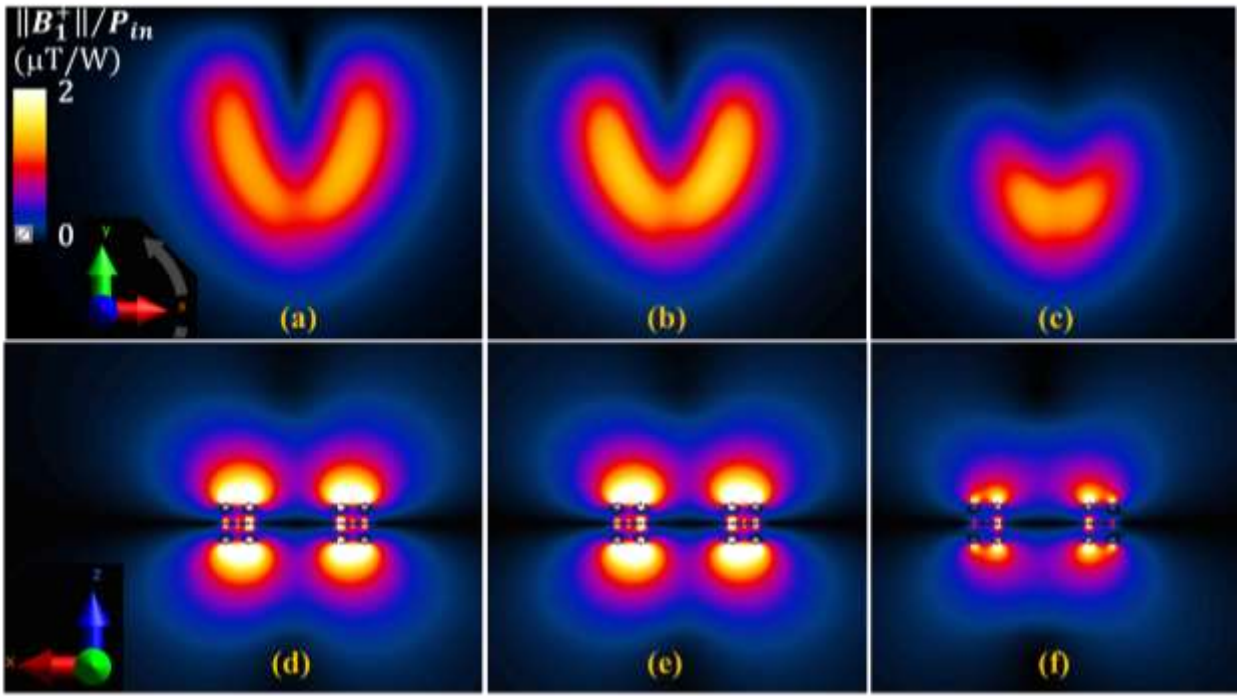

Supporting Information Figure S10: Dipoles constructed with different sizes have similar sensitivity distributions. Transverse slices at z=20mm from ||B1+|| maps of the homogeneous phantom with (a) large, (b) medium, and (c) small size multi-planar dipoles with shorted ends and high permittivity cover. Coronal slices across the center of the dipole arms for (d) large, (e) medium, and (f) small size dipoles.

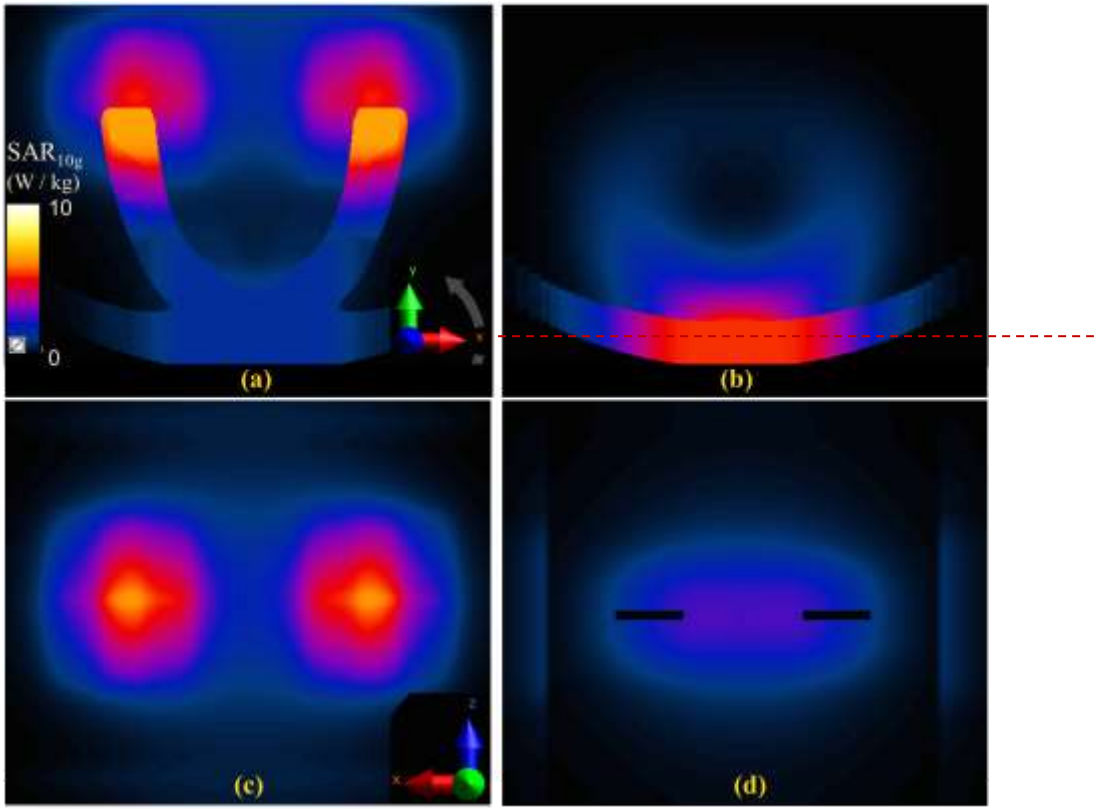

Supporting Information Figure S11: Transverse slices at z=10mm from SAR_{10g} maps of the homogeneous phantom with (a) dipole and (b) the loop coil. Highest SAR_{10g} for the dipole is observed at the high permittivity section of the dipole arms and around the end of the arms as shown in (c) the coronal slice, whereas for the loop, the feed port region has the highest SAR. (d) A coronal view from the SAR_{10g} map of the loop coil along the dashed line shown in (b).

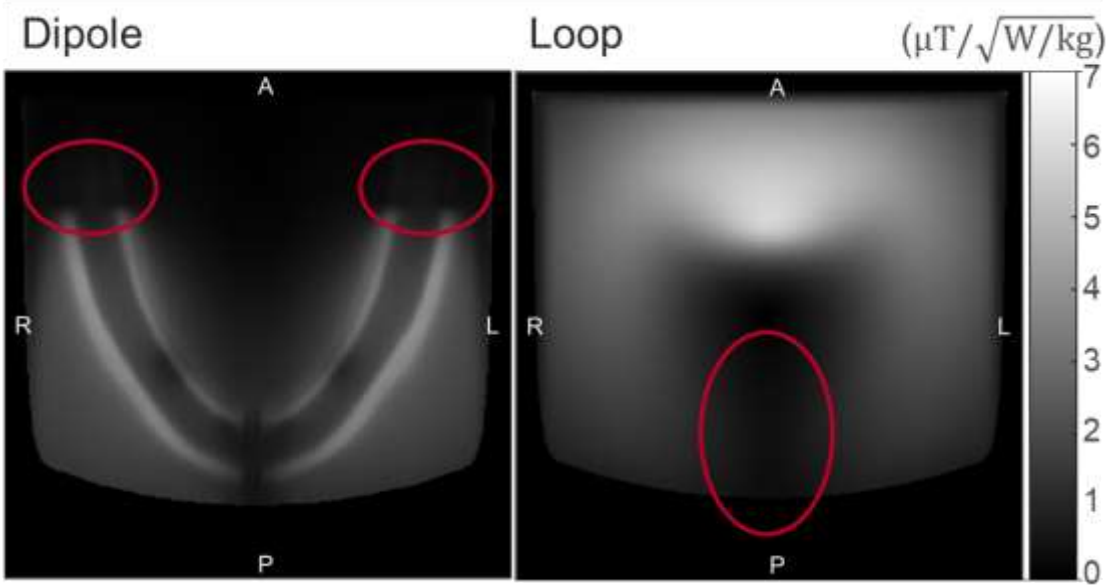

Supporting Information Figure S12: SAR efficiency maps of the homogeneous phantom using dipole and the loop coil. SAR efficiency of the dipole drops at the end of the dipole arms (marked with red ovals), where high permittivity section begins. The loop coil has the maximum SAR efficiency at the distal conductor and the minimum SAR efficiency around the feed port (marked with red oval).

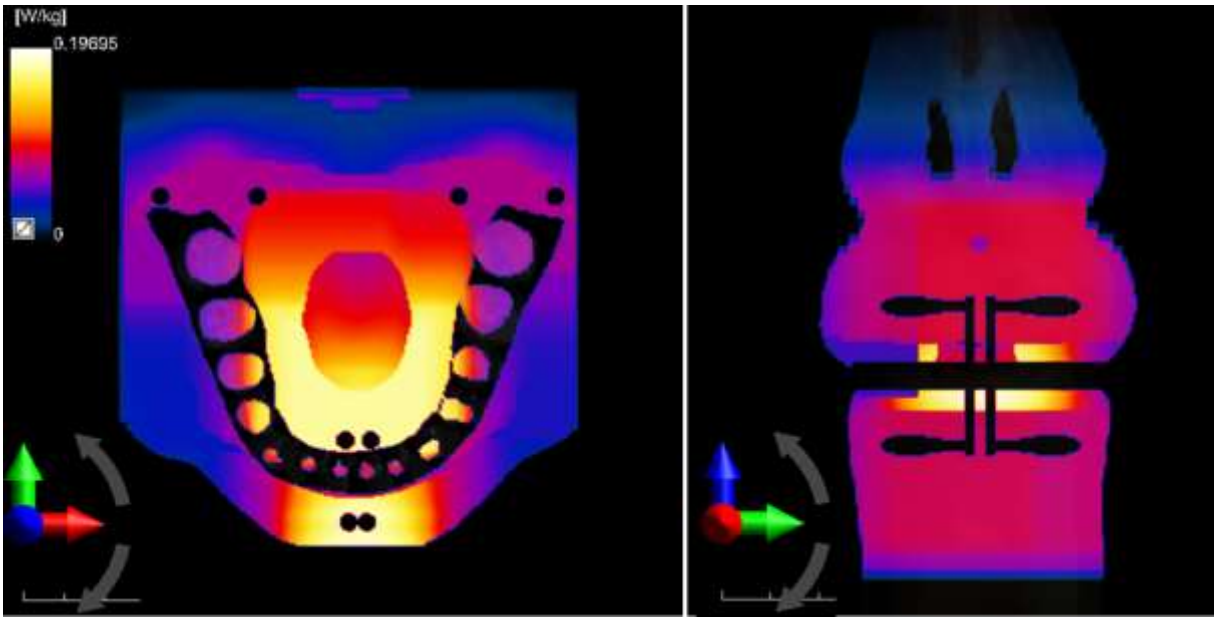

Supporting Information Figure S13: SAR_{10g} maps in Duke anatomical model for the intraoral dipole without the high ε_r section at the end of the dipole arms in transverse (left) and coronal planes (right). The planes are selected with the maximum values, and the color bars also represent the dynamic range of the SAR_{10g} maps.

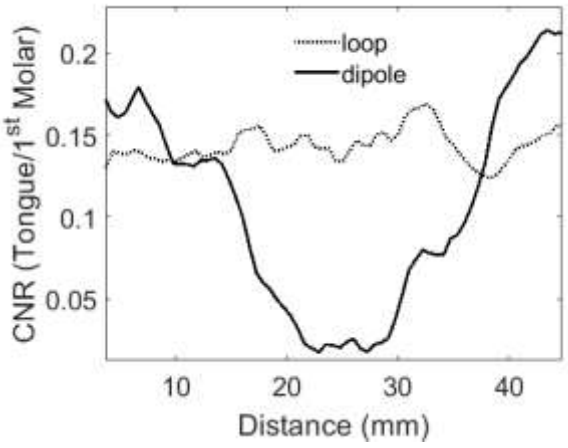

Supporting Information Fig. S14: Comparison of contrast-to-noise ratio (CNR) of signal from the tongue and signal from the first molar tooth for loop and dipole along the line profiles indicated in Fig. 10e, f. Signal from tongue is suppressed significantly around the medial sulcus of the tongue, yet the edges are still prominent due to gradual decrease of the dipole sensitivity towards the center of the tongue.

Pulse sequence protocols

B1 mapping

ScanningSequence:	GR
SequenceVariant:	SP
ScanOptions:	PFP
MRAcquisitionType:	2D
SequenceName:	*fl2d1
AngioFlag:	N
SliceThickness:	4
RepetitionTime:	4000
EchoTime:	3
NumberOfAverages:	1
ImagingFrequency:	123.190.667
ImagedNucleus:	1H
EchoNumber:	1
MagneticFieldStrength:	3
NumberOfPhaseEncodingSteps:	4
EchoTrainLength:	96
PercentSampling:	1
PercentPhaseFieldOfView:	100
PixelBandwidth:	280
DeviceSerialNumber:	67024
SoftwareVersion:	E11
ProtocolName:	2D_GRE_IOL_SRFExc2V
TransmitCoilName:	H1TR
AcquisitionMatrix:	128\0\0\128
InPlanePhaseEncodingDirection:	COL
FlipAngle:	5
VariableFlipAngleFlag:	N
SAR:	0.0042
dBdt:	0
PatientPosition:	HFS

Instead of flip angle, the amplitude of the voltage at the output of the RFPA was set. For the body coil excitation, 15V and 30V were entered, for the intraoral coils, 2V and 4V assuming that these voltage levels would result in a small flip angle required for the double angle B1 mapping method.

3D GRE

SequenceName:	'*fl3d1'
AngioFlag:	'N'
SliceThickness:	0.6
RepetitionTime:	25
EchoTime:	3.14
NumberOfAverages:	1
ImagingFrequency:	123.1905
ImagedNucleus:	'1H'
EchoNumber:	1
MagneticFieldStrength:	3
NumberOfPhaseEncodingSteps:	192
EchoTrainLength:	1
PercentSampling:	100
PercentPhaseFieldOfView:	100
PixelBandwidth:	280
DeviceSerialNumber:	'67024'
SoftwareVersion:	'syngo
ProtocolName:	'3D_GRE_06iso_allRx'
TransmitCoilName:	'H1TR'
AcquisitionMatrix:	256*256*144
InPlanePhaseEncodingDirection:	'COL'
FlipAngle:	30
VariableFlipAngleFlag:	'N'
SAR:	0.0043
dBdt:	0
PatientPosition:	'HFS'

UTE

ScanningSequence	GR
SequenceVariant	SP
ScanOptions	
MRAcquisitionType	3D
SequenceName	fl3d2_ns
AngioFlag	N
SliceThickness	0.859375
RepetitionTime	7.96
EchoTime	0.06
NumberOfAverages	1
ImagingFrequency	123.190455
ImagedNucleus	1H
EchoNumbers	1
MagneticFieldStrength	3
NumberOfPhaseEncodingSteps	65535
EchoTrainLength	0
PercentSampling	100
PercentPhaseFieldOfView	100
PixelBandwidth	450
DeviceSerialNumber	67024
SoftwareVersions	syngo MR E11
ProtocolName	ute_65535_allRx
TransmitCoilName	H1TR
AcquisitionMatrix	128\0\0\128
InPlanePhaseEncodingDirection	COL
FlipAngle	6
VariableFlipAngleFlag	N
SAR	0.001154892
dBdt	0
PatientPosition	HFS

Simulation Settings

Simulation Settings	EM FDTD DUKE	EM FDTD Homogeneous phantom
Preparation		
Type	*EM-FDTD Single-port simulation*	*EM-FDTD Single-port simulation*
Setup		
Simulation Time	15 Periods	15 Periods
Global Auto Termination	Medium	Medium
Materials		
Phantom/Gel	NA	Dielectric
		er = 78
		s = 0.47 S/m
		c=1000kg/m3
Conductors	PEC	PEC
Isolation	Dielectric	Dielectric
	er=3.2	er=3.2
	c=1000kg/m3	c=1000kg/m3
High permittivity coating	Dielectric	Dielectric
	er=270	er=300
	c=1000kg/m3	c=1000kg/m3
Sources		
Type	1xEdge port	1xEdge port
Excitation signal	Harmonic/Gaussian for broadband simulation	Harmonic/Gaussian for broadband simulation
Frequency	123MHz/120MHz span	123MHz/120MHz span
Reference Load Port 1	12-27Ohms extracted from broadband sim.	12-27Ohms extracted from broadband sim.
Lumped elements		
Element type	Inductor/ capacitor for loop coil	Inductor/ capacitor for loop coil
Value	15nH/15.18pF for loop	15nH/ 14.5pF for loop
Sensors		
Number of edge sensors	3	3
Auto termination	Use global	Use global
Sampling	51	51
Number of field sensors	1	1
Record domain	Frequency domain	Frequency domain
Fields recorded	E- and H-field	E- and H-field
Boundary conditions		
Type	ABC	ABC
Strength	Medium	Medium
Grid	305x317x163	373x369x162
	15.7 Mcells	22.2 MCells
Solver		
Parallelization handling	Automatic	Automatic
Kernel	CUDA	CUDA
Solver mode	FDTD	FDTD

Supplementary Video Files

Two video files are uploaded separately:

Supporting Information Video S1: Animated view of the transverse slices of the transmit efficiency map of the meandered intraoral dipole.

Supporting Information Video S2: Animated view of the transverse slices of the in vivo GRE and UTE images acquired with the loop coil, dipole, dipole and SLR combination.